Egyptian Journal of Chemistry

http://ejchem.journals.ekb.eg/

Determination of Ferrous Ion in Pure & Pharmaceutical Preparation by Continuous Flow Injection Analysis Via Turbidmetric Utilizing NAG-4SX3-3D Analyzer

Sarah Faris Hameed and Nagham Shakir Turkie*

Department of chemistry, College of science, University of Baghdad, Baghdad, Iraq

Abstract

A simple and efficient established method that is characterized by its quickness and high sensitivity for determining ferrous ion in pure and pharmaceutical formulations by generate of dark-blue precipitate using reaction of hexacyanoferrate(III) with ferrous ion in ammonium acetate medium. The equipment NAG-4SX3-3D analyzer was used to quantify turbidity by measuring the incident light attenuation crashing on the precipitate surface granules (0-180 degree). The optimum parameter has been investigated in order to improve the newly created approach's sensitivity.

The linear range (0.1-7) mmol.L^{-1} with (r=0.9971), (correlation coefficient), percentage linearity (R % = 99.42), and RSD % for the repetition (n=7) also were lower than 0.1 percent for the measurement of ferrous ion, with concentration (1, 4.7 mmol .L^{-1}). Whereas L.O.D. = 212.6712 ng/sample from the progressive dilution throughout the calibration graph's lowest concentration linear dynamic range the suggested approach was compared to the traditional method (UV- spectrophotometric at λ_{max} = 222 nm of analysis employing the conventional technique of adding by the use of paired t- test (the mean difference between pairs of measurements). It's noticed that with calculated numbers, there wasn't any substantial variation between the values given of any particular firm, t-value at 95% interval from the proposed approach.

***Key word*:** Fe (II); turbidity; flow injection analysis ;hexacyanoferrate; Turnbull's blue.

1. Introduction

Iron "Fe" is a micronutrient that is required by practically all living things [1]. In photosynthesis and respiration, Chlorophyll generation, nitrate reduction and reactive oxygen species detoxification are just a few of the metabolic activities iron participates and electron transport [2]. Due to its poor solubility, Fe concentrations in natural water sources range from 10-8 mmol in river water to 10-9 mmol in coastal water and 10-13 mmol in ocean water [3]. Ferrous and ferric, the total Fe pool includes both organic and inorganic complexes, colloidal Fe and particulate Fe. Iron is also important to living organisms since it serves as a cofactor for several enzymes[4,5] , including catalase, cytochrome and peroxidase. It is also required for the transport of oxygen and the transfer of electrons. Iron has been established to have a daily dosage of 0.8 mg per kilogram of body weight and at excessive amounts, it can be poisonous [6, 7]. Excess iron causes cancer, organ damage, skin and muscular problems, while iron shortage causes anemia [8]. As a result, identifying trace quantities of iron is critical in order to safeguard the environment and avoid harmful health impacts from iron accumulating in organs and tissues. There are several analytical methods used to determinate the amount of iron such as flame atomic absorption spectrometry (FAAS) [9], inductively coupled plasma optical emission spectrometry [10], inductively coupled plasma mass spectrometry [6], digital image colorimetric [11], atomic absorption spectrometry [12, 13], liquid-liquid micro extraction [14], spectrophotometry [15] , in situ solvent formation micro extraction (ISFME)[16-18] ,chemiluminuteescence- continuous flow injection analysis[19] etc.

The current investigation was based on the reaction of ferrous ion with potassium hexacyanoferrate (III) to form a blue precipitate using a newly homemade NAG-4SX3-3D analyzer [20-22], for determination of ferrous ion in pure and pharmaceutical preparations.

*Corresponding author e-mail: *sarahf.hameed@yahoo.com*.; (Sarah Faris Hameed).

Receive Date: 03 April 2022, **Revise Date:** 30 April 2022, **Accept Date:** 17 May 2022, **First Publish Date:** 17 May 2022
DOI: 10.21608/EJCHEM.2022.131307.5788

2. Chemicals and Apparatus

2.1. The reagents and the Chemicals utilized

Chemicals of analytical grade reagents were applied in all of the experiments. Ferrous ion 0.25mol.L^{-1} (FLUKA, Germany) was made by dissolving 24.5088 g (250ml) of $FeSO_4.7H_2O$ in distilled water in a little quantity then add 10 ml of concentrated H_2SO_4 (in order to avoid transform ferrous ion to ferric ion) followed by the addition of distilled water to the mark. Potassium hexacyanoferrate (III) K_3 $[Fe(CN)_6]$ 0.25mol.L^{-1} (BDH, UK) was made by dissolving 41.1575 g in 500mL of distilled water.

2.2 Apparatus

The resultant output from the attenuation of incident light (0-180°) was accumulated using a flow cell manufactured from a handmade NAG-4SX3-3D analyzer. A potentiometric recorder (Siemens, Germany) was used to record the output signals. Ismatic peristaltic pump and six-port injection valve with sample loop (Teflon, variable length). For the conventional approach, an UV spectrophotometric (Shimadzu, Japan) was employed.

3. Methodology

Flow injection manifold system for the reaction of ferrous ion with potassium hexacyanoferrate (III) to form a dark- blue precipitate [23-24] was studied, coupled with a homemade NAG-4SX3-3D analyzer, which is shown in figure .1.A

The study has been carried out using experimental conditions, 4 mmol.L^{-1} of Fe (II) with 139µL as a sample volume, 20 mmol.L^{-1} of $K_3[Fe(CN)_6]$ and flow rate 2.8 ml.min^{-1} for carrier (H_2O) and reagent $K_3[Fe(CN)_6]$. The carrier stream line (H_2O) passing through the 6-port injection value carrying the sample Fe(II) Ion 4 mmol.L^{-1}. The carrier stream line will mix with the reagent line at a Y- junction to form blue precipitate leading to measured response via NAG-4SX3-3D Analyzer as shown in figure .1.A. figure .1.B shows profile of preliminary experiment for assessment of NAG-4SX3-3D. The reaction mechanism is as follows in scheme (1)

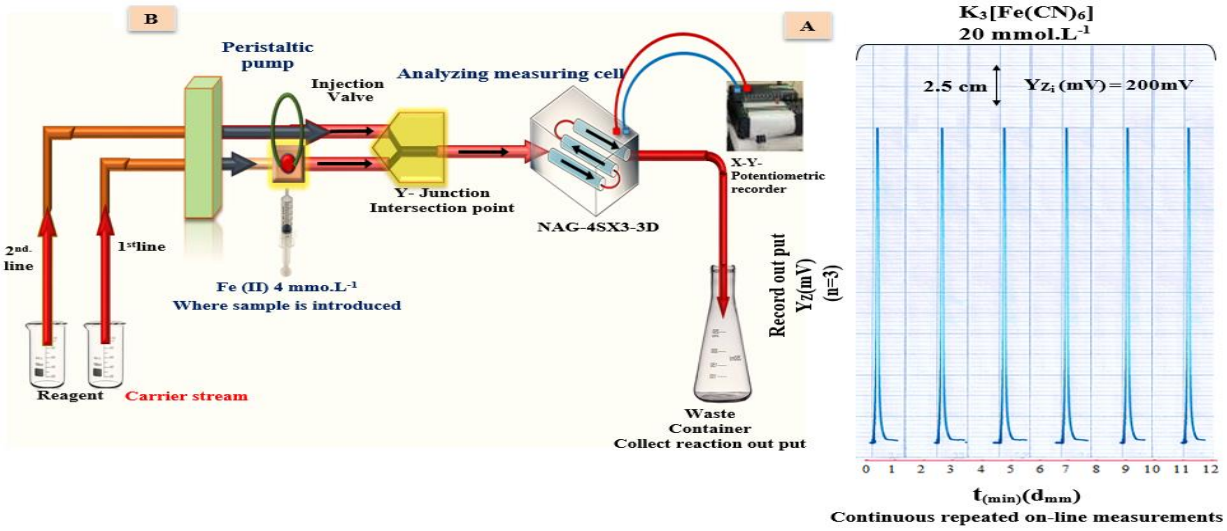

Fig.1.A: Diagram of manifold used for assessment NAG-4SX3-3D via reaction of Fe(II) ion 40 mmol.L^{-1} with Potassium hexacyanoferrate (III) 20 mmol.L^{-1} to form Turnbull's blue. B: Profile of preliminuteary experiment for assessment NAG-4SX3-3D via reaction of Fe(II) ion with Potassium hexacyanoferrate (III) to form Turnbull's blue.

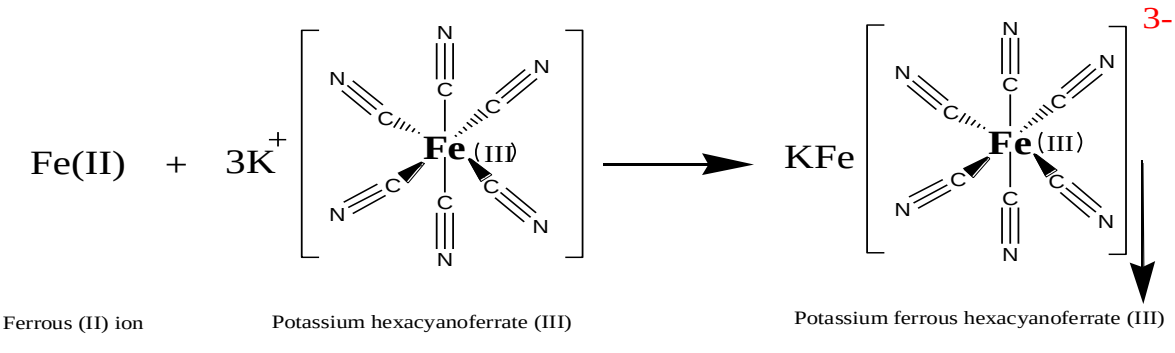

Scheme (1): The reaction for precipitate formation

4. Result and Discussion

The flow injection manifold system (figure. 1.A) was used to investigate chemical and physical factors in order to identify the conditions for generation the reaction product Turnbull's blue precipitate with the highest repeatability and sensitivity possible. These variables were optimized by keeping all of them constant while changing one at a time.

4. A. Chemical variables

4 .A.1.Effect of variable concentration of [$K_3Fe(CN)_6$]

The effect of varying concentration of $K_3[Fe(CN)_6]$ as a precipitating reagent was carried out using a range of solutions (10-55) mmol. L^{-1} and 2.8 $mL.min^{-1}$ flow rate for each line. Constant concentration of Fe (II) Ion (4$mmol.L^{-1}$) was used with 139 µL as sample volume. Table 1.A summarized and presented obtained results; such as relative standard deviation and confidence interval , it demonstrates that an increase in $K_3[Fe(CN)_6]$ concentration leads to increase in the attenuation the incident light on the precipitate particle surface up to 40 $mmol.L^{-1}$, after this concentration there had been a decrease in the attention of the incident light in mV, this might be owing to the non-accumulation impact of precipitate particles causing a decrease in granule density. So, 40 $mmol.L^{-1}$ $K_3[Fe(CN)_6]$ concentration was selected as the optimal concentration for future investigation. Searching is made to find for highest intercept and lowest or acceptable slope, correlation coefficient and angle value were investigated. The 3-point plot shown that the segment S_4 (40-55) $mmol.L^{-1}$, the most acceptable regions to select. While the rest of segments shows low sensitivity. Table1.B. shown data point within the range can be chosen.

4. A.2. Type of media effect (salt and acid)

The reaction of Fe(II) ion (4$mmol.L^{-1}$)-$K_3[Fe(CN)_6]$ (40 $mmol.L^{-1}$) system was investigated in variable media (acid and salt) at (50 $mmol.L^{-1}$) concentration additionally aqueous media(distilled water), flow rate 2.8 $ml.min^{-1}$ for each line and sample volume 139 µL. The data obtained was plotted in the diagram below. Figure. 2.A, B, in which with varied media, the variations in the energy response of the transducer is given peak heights on average (n = 3) in mV, and response profile. It was found that ammonium acetate was the suitable as a carrier stream for maximum attenuation of the incident light compared to the use of different acids, salts and distilled water. Most likely as a result of an increase in the amount of precipitate particles. due to the present of ammonium acetate that may work as a catalyst for precipitate formation.

4. A.3. Effect of Ammonium acetate salt concentration

Using Fe(II) ion (4 $mmol.L^{-1}$) – $K_3[Fe(CN)_6]$ (40 $mmol.L^{-1}$) system. Varying concentrations of ammonium acetate (10-60) $mmol.L^{-1}$ were prepared, 139 µL as sample volume and flow rate 2.8 $ml.min^{-1}$ for both carrier stream and reagent. From table below, it was discovered that a rise in peak height was associated with an increase in ammonium acetate concentration, which might be attributable to an increase in precipitate granules. Therefore, 50 $mmol.L^{-1}$ was selected as the optimal concentration up to 50 $mmol.L^{-1}$, S/N-transducer response is reduced as a result. Because some of the precipitate particles' solubility has decreased..

Table 1.A: Effect of potassium hexacyferrate (III) concentration on precipitation of Fe(II) ion, B:Segmentation pattern intercept –slope, correlation coefficient and angle with selected the optimum segment of Fe(II) ion-$[Fe(CN)_6]^{-3}$ system

A			
$[Fe(CN)_6]^{-3}$ $mmol.L^{-1}$	$\bar{Y}_{Zi}$(mV) overall average (n=3)	RSD%	Confidence level at 95 % $\bar{Y}_{Zi}$(mV)± t SEM
10	1200	0.11	1200±3.279
20	1520	0.08	1520±3.006
30	1648	0.10	1648±4.074
40	1736	0.06	1736±2.785
50	1568	0.07	1568±2.608
55	1160	0.11	1160±3.180

B					
Segment	$[Fe(CN)_3]^{-3}$ range mmol. L^{-1}	Intercept mV	Slope mV/ $mmol.L^{-1}$	correlation coefficient (r)	Angle (tangent)
S_1	10-30	1008.00	22.40	0.9707	87.444
S_2	20-40	1310.67	10.80	0.9943	84.710
S_3	30-50	1810.67	- 4.00	-0.4760	-75.964
S_4	40-55	3194.86	-35.31	-0.9105	-88.378

$\bar{Y}_{Zi}$(mV):(S/N) energy transducer in mV, $t_{0.025,2}$=4.303.

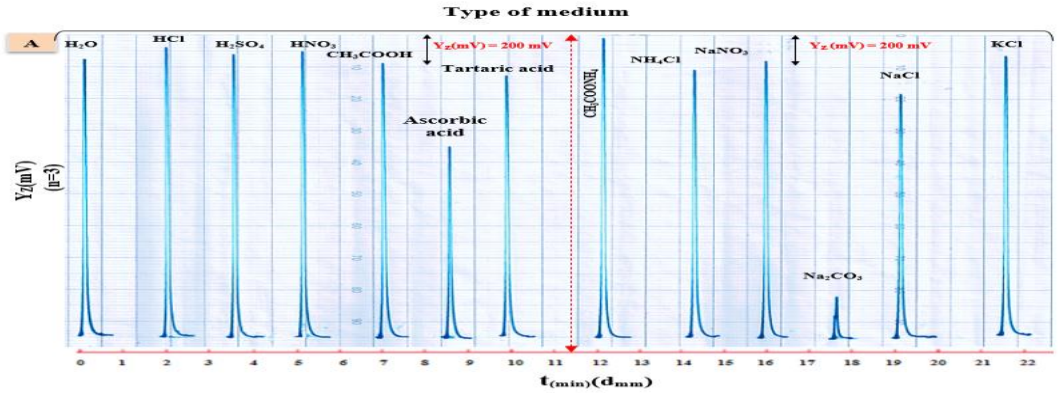

Fig.2.A: Effect type of medium (salt & acid) on A: Response profile Y_Z- $t_{(minute)(dmm)}$

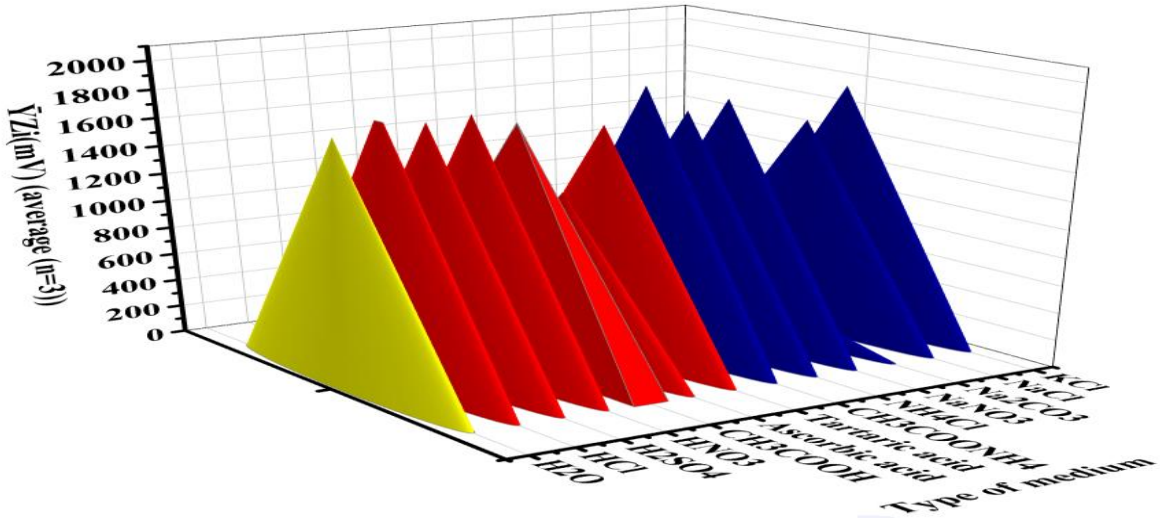

Fig.2.B: Transducer attenuation response for the assessment of NAG-4SX3-3D via formation of Turnbull's blue

Table 2.A: Effect of variation ammonium acetate concentration on precipitation of Fe(II) ion, B: Segmentation pattern intercept -slope, correlation coefficient and angle with selected the optimum segment of Fe(II) (4mmol.L^{-1})-$[Fe(CN)_6]^{-3}$ (40 mmol.L^{-1}) system

A				
$[CH_3COONH_4]$ mmol.L^{-1}	**$\bar{Y}_{Zi}$(mV) overall average, (n=3)**	**RSD%**	**Confidence level at 95 % $\bar{Y}_{Zi}$(mV)± t SEM**	
10	**1784**	**0.10**	**1784± 4.422**	
30	**1776**	**0.07**	**1776±3.279**	
40	**1792**	**0.08**	**1792±3.602**	
50	**1872**	**0.06**	**1872±3.006**	
60	**1696**	**0.10**	**1696±4.298**	
B				
Segment	**$[CH_3COONH_4]^{-3}$ mmol.L^{-1}**	**Intercept mV**	**Slope mV/ mmol.L^{-1}**	**correlation coefficient(r)**	**Angle (tangent)**
S_1	**10-40**	**1779.43**	**0.17**	**0.3273**	**9.728**
S_2	**30-50**	**1621.33**	**4.80**	**0.9333**	**78.232**
S_3	**40-60**	**2026.67**	**- 4.80**	**-0.5447**	**-78.232**

$\bar{Y}_{Zi}$(mV):(S/N) energy transducer in mV, $t_{0.025,2}$=4.303

Most of the particles will be in the form of big sized particulate, mainly it could not be in the form of nucleus which in turn not to collect in its packed blocked form and that will not help in agglomeration causing a decrease of attenuation of incident light. The results corresponding with slope-intercept-correlation coefficient and angle calculation (table 2.B), S_3 is a category in which the segment of choice can be made (i.e.;40-60 mmol.L^{-1}). The selected segment contains 50 mmol.L^{-1}

4. B. Physical variables

4. B.1.Effect of flow rate

The flow rate of the carrier stream was optimized through a series of studies. (ammonium acetate) 50 mmol.L^{-1} and reagent stream $K_3[Fe(CN)_6]$ 40mmol.L^{-1} using (4 mmol.L^{-1}) at 139 µL as sample volume . As demonstrated in figure.3.A, there was an increase in dilution and dispersion at low flow rates, which might lead to an increase in peak base width (Δt_B). To achieve a maximal reaction, a flow rate of 2.5ml.min^{-1} was employed for both the carrier and reagent streams. Figure.3.A is showing variation of flow rate versus S/N energy transducer output response profile of NAG-4SX3-3D analyser. The result obtained were tabulated in table 3.A. On the basic of intercept – slope correlation coefficient and angle, This might be seen in table 3.B and figure.3.B in which that section is S_4 (i.e.; 2.5-3 ml.min^{-1}) was the optimum and 2.5 ml.min^{-1} ,the optimal flow rate for both the carrier and reagent streams was discovered within the designated segment and was employed in further trials.

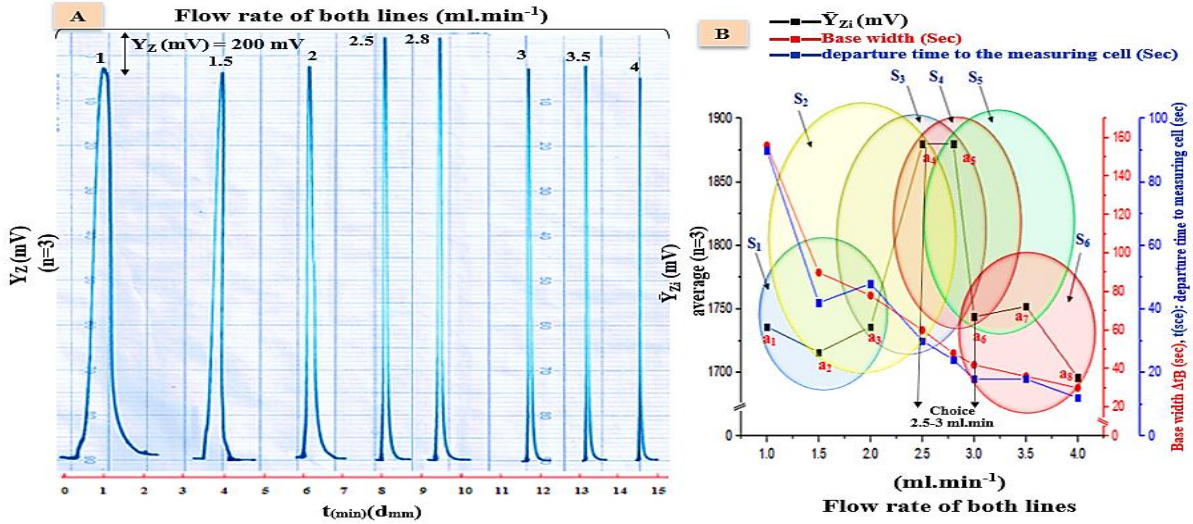

Fig.3. A: Response profile of effect flow rate on transducer attenuation response for the assessment of NAG-4SX3-3D via formation of Turnbull's blue. B: $\bar{Y}_Z$ (mV) output of (S/N) energy transducer response and three data point as one segment with optimum choice

Table 3.A: Effect of flow rate variation on precipitation of Fe(II), B: Segmentation pattern intercept –slope, correlation coefficient and angle with selected the optimum segment of Fe(II) ion (4mmol.L^{-1})-$[Fe(CN)_6]^{-3}$(40 mmol.L^{-1})- $[CH_3COONH_4]$ (50 mmol.L^{-1}) system, at 139 µL sample volume.

A									
Pump speed	Flow rate ml.min^{-1} for each line	$\bar{Y}_{Zi}$(mV) overall average (n=3)	RSD%	Confidence level at 95% $\bar{Y}_{Zi}$(mV)± t SEM	Δt_{sec}	V_{add} (ml) at flow rate	C (mmol.L^{-1})	D.F	t_{sec}
5	1.0	1736	0.05	1736±2.062	156	5.339	0.104	38.4101	90
10	1.5	1716	0.07	1716±3.006	90	4.639	0.120	33.3741	42
15	2.0	1736	0.08	1736±3.354	78	5.339	0.104	38.4101	48
20	2.5	1880	0.05	1880±2.534	60	5.139	0.108	36.9712	30
25	2.8	1880	0.08	1880±3.602	48	4.619	0.120	33.2302	24
30	3.0	1744	0.07	1744±3.155	42	4.339	0.128	31.2158	18
35	3.5	1752	0.08	1752±3.279	36	4.339	0.128	31.2158	18
40	4.0	1696	0.10	1696±4.174	30	4.139	0.134	29.7770	12

B					
Segment	Flow rate ml.min^{-1}	Intercept mV	slope mV/ mmol.L^{-1}	correlation coefficient (r)	Angle (tangent)
S_1	1-2	1729.33	0.00	0.00	0.00
S_2	1.5-2.5	1449.33	164.00	0.916	89.651
S_3	2-2.8	1367.18	191.02	0.929	89.700
S_4	2.5-3	2527.79	-250.53	- 0.803	-89.771
S_5	2.8-3.5	2240.31	-144.62	- 0.683	-89.604
S_6	3-4	1898.67	-48.00	- 0.792	-88.807

$\bar{Y}_{Zi}$(mV):(S/N) response of energy transducer in mV, $t_{0.025,2}$=4.303, Δt_{sec} :Base width of peak (second), t_{sec} : the dewatering time from the injection valve into metering cell, C : Concentration, Df : Dilution factor at flow cell

4.B.2. Effect of sample volume

Using the most effective parameters discovered in previous studies. The sample volume effect (Fe (II) ion 4 mmol. L^{-1}) as analyte was used. Different length of teflon tube (10.4-35.8 cm) of diameter 0.5 mm was utilized to determine the best sample volume to use throughout the procedure. The result obtained were listed in table 4.A. it was observed that, the increase of the base width (Δt_B) with increasing the length of sample volume. Due to the considerable time it takes for the carrier stream to pass through the injection valve, the flow is restricted, resulting in an increase in the dispersion of precipitate particles segment and a rise in the base width (Δt_B). A compromise in this study was made to chosen 175 µL as suitable most convenient of sample volume. On the basis of intercept – slope – correlation coefficient and angle calculation which is shown in table 4.B in which that segment S_4 (i.e.; 141-281 µL) was the chosen segment and 175 µL with in the chosen segment was the optimum sample volume and will be used for further experiments.

Table 4.A: Effect of the sample volume variable on precipitation of Fe (II) ion. B: Segmentation pattern intercept–slope, correlation coefficient and angle with selected the optimum segment of Fe(II) (4mmol.L^{-1})-$[Fe(CN)_6]^{-3}$(40 mmol.L^{-1})- CH_3COONH_4 (50 mmol.L^{-1}) system at 2.5 ml.min^{-1} flow rate for each line

A									
Length of sample segment cm r= 0.5	Sample volume µL	$\bar{Y}_{Zi}$(mV) overall average , (n=3)	RSD%	Confidence level at 95% $\bar{Y}_{Zi}$(mV)± t SEM	Δt_{sec}	V_{add} (ml) at flow rate	C (mmol.L^{-1})	D.F	t_{sec}
10.4	82	1080	0.11	1080±3.080	50	4.249	0.077	51.813	24
14.6	115	1552	0.10	1552±3.900	54	4.615	0.100	40.130	27
17.7	139	1880	0.06	1880±3.006	59	4.917	0.110	36.372	31
18	141	1960	0.08	1960±3.677	63	5.391	0.105	38.234	34
22.3	175	2020	0.08	2020±4.149	64	5.508	0.127	31.476	36
35.8	281	2320	0.09	2320±4.919	65	5.698	0.197	20.276	37

B					
Segment	Sample volume µL	Intercept mV	slope mV/ mmol.L^{-1}	correlation coefficient(r)	Angle (tangent)
S_1	82-139	-69.74	14.05	0.9999	85.929
S_2	115-141	-156.70	14.84	0.9932	86.145
S_3	139-175	1506.24	2.95	0.8491	71.626
S_4	141-281	1576.00	2.63	0.9969	69.2046

$\bar{Y}_{Zi}$(mV):(S/N) energy transducer in mV, $t_{0.025,2}$=4.303, Δt_{sec} :Base width of peak (sec), t_{sec} : the dewatering time from the injection valve into metering cell, 0*: Without coil, C: Concentration, Df : Dilution factor at flow cell.

4. B.3. The impact of a delay reaction coil on the S/N response curve

Table 5.A: Effect of the variation of reaction coil on precipitation of Fe (II) ion. B: Segmentation pattern intercept–slope, correlation coefficient and angle with selected the optimum segment of Fe (II) (4mmol.L^{-1})-$[Fe(CN)_6]^{-3}$(40 mmol.L^{-1})- CH_3COONH_4 (50 mmol.L^{-1}) system at 2.5 ml.min^{-1} flow rate for each line and 175µL sample volume.

A									
Coil length Centimeter r=1 mm	**Coil length µL**	**$\bar{Y}_{Zi}$(mV) overall average , (n=3)**	**RSD%**	**Confidence level at 95% $\bar{Y}_{Zi}$(mV)± t SEM**	**Δt_{sec}**	**V_{add} (ml) at flow rate**	**C (mmol.L^{-1})**	**D.F**	**t_{sec}**
Without	**0**	**2020**	**0.05**	**2020± 2.584**	**63**	**5.425**	**0.129**	**31.000**	**35**
10	**314**	**1860**	**0.07**	**1860±3.006**	**64**	**5.333**	**0.127**	**31.000**	**40**
20	**628**	**1880**	**0.08**	**1880±3.602**	**65**	**5.592**	**0.125**	**31.952**	**45**
25	**785**	**1800**	**0.09**	**1800±4.174**	**66**	**5.675**	**0.123**	**32.429**	**50**
30	**942**	**1780**	**0.11**	**1780±4.695**	**67**	**5.758**	**0.122**	**32.905**	**56**

B					
Segment	**Coil length µL**	**Intercept mV**	**slope mV/ mmol.L^{-1}**	**correlation coefficient (r)**	**Angle (tangent)**
S_1	**0-785**	**1992.54**	**-0.24**	**- 0.8881**	**- 13.360**
S_2	**314-942**	**1922.29**	**-0.14**	**- 0.7789**	**- 7.875**

$\bar{Y}_{Zi}$(mV):(S/N) energy transducer in mV, $t_{0.025,2}$=4.303, Δt_{sec} :Base width of peak (sec), t_{sec} : the dewatering time from the injection valve into metering cell, C: Concentration, Df : Dilution factor at flow cell.

Fe(II) ion (4 mmol.L $^{-1}$) and $K_3[Fe(CN)_6]$ (40 mmol.L $^{-1}$) system was used. 175 µL as the injection sample volume and flow rate 2.5 ml.min^{-1} for carrier stream (ammonium acetate 50 mmol.L^{-1}) and reagent stream. At variable coil length (0, 314, 628, 785, and 942) µL as shown in table 5.A reaction coil attached after Y- junction. The purpose in why conducing this study is because of having the rearrangement of precipitate particles. As a result, it was observed that utilizing variable volume (different length of reaction coil) will result in dilution of sample zone reaction product, resulting in a distribution when using a very high volume, resulting in a highly dispersed of precipitate, resulting in a weaker signal because sample zone takes longer time duration of precipitate species in front of the detector, as shown in table 5. A. Therefore; there was no need to connect a coil between Y- junctions to measuring cell. On the basis of slope- intercept, correlation coefficient and angle which might be seen in table 5.B in which that segment S_1 (i.e.; 0-785 µL) was the optimum and 0 µL (without reaction coil) , the optimal delay response coil was found inside the designated segment and was utilized in further testing.

5. The effect of Fe (II) ion concentration on the output of energy transducers of divergent light

Under the established optimum chemical and physical variables, a series of Fe (II) ion solutions (0.1-25) mmol.L^{-1} were prepared; it's what the X-axis will look like "Independent variable". The attenuation of incident light was measured using the NAG-4SX3-3D, which produced S/N energy transducer responses as Y-"represent the dependent variable" as shown in figure.4.A, with the peak height of response increasing as the concentration of analyte rose. Figure 4.C depicts a profile. Its represented by scatter–plot at range (0.1-25) mmol.L^{-1} (i.e. All twenty points were chosen with the correlation coefficient r = 0.8592 as shown in table 6 a rise in Fe(II) ion concentration induces an increase in precipitate particles, according to the analytical range. Up to 10 mmol.L^{-1}, a broad in maxima of peak height was noticed, because an increase of precipitate particles , as a consequence of the decrease in interstitial gaps and reflecting surface, as well as the increase in particle size, particles move slowly, resulting in a prolonged time duration of particles in front of the detector, resulting in a distorted response. Figure.4.B. Analytical range (dynamic range) (0.1-15) mmol.L^{-1} (n=18) with r =0.9342, working range (0.1-10) mmol.L^{-1} (n=17) with r =0.9874 and linear range (linear dynamic range) (0.1-7) mmol.L^{-1} (n=16) with r =0.9973.

To enhance the assessment of mathematical formulations, a shorter range should be chosen while looking for a better representation. Table 6 tabulates all the results obtained that covers the calibration range including the correlation coefficient, coefficient of determination, percentage capital R- squared and t-table. With r = 0.9973 and R%=99.45, the best linear equation for the relationship between Fe (II) ion concentration and divergent light exists. On the form:

$\hat{Y}_{Zi}$(mV)=24.816±82.3918=539.9350±22.9292 [Fe (II)] mmol.L^{-1}

The output of the scatter plot was able to articulate the acquired results from n=16. The development of the developed strategy for determining Fe (II) ion was compared to the traditional method (reference method) [19] namely UV-spectrophotometric method that based on the absorbance measurements at λ_{max}= 222 nm as show in table 6. The best linear ranging from 0.1 to 3.5 mmol.L^{-1} of n=11 with correlation coefficient of 0.9971 and R% = 99.43 (table 6).

Table 6: Summary of linear regression data for the variations of the (S/N) energy transducer response with Fe (II) ion concentration using the first degree equation of the form $\hat{Y}$=a+ b x at optimum conditions

Type of mode	Range of [Fe (II)] ion mmol.L^{-1}(n)	$\hat{Y}_{Z\,i}$=a ± S_a t+b(Δ y /$\Delta x_{mmol/L}$) ± S_b t [Fe (II)] mmol.L^{-1} at confidence level 95%, n-2	r, r^2, R^2%	t_{tab} at 95%, n-2	Calculated t-value t_{cal}=/r/√n-2 / √1-r^2
Developed method using NAG - 4SX3 - 3D analyser					
UV- Spectrophotometer at λ_{max}= 222nm.					
Linear range or linear dynamic range	0.1-7 (16)	24.8160±82.3918+539.9350±22.9292 [Fe (II)] mmol.L^{-1}	0.9973, 0.9945, 99.45	2.145 << 50.510	
	0.1-3.5 (11)	-0.0222±0.0527+0.5087±0.0291 [Fe (II)] mmol.L^{-1}	0.9971,0.9943, 99.43	2.262 << 39.455	
Working range or calibration range	0.1-10 (17)	158.3580±180.7623+481.8330±42.5651 [Fe (II)] mmol.L^{-1}	0.9874,0.9749, 97.49	2.131 << 24.123	
	0.1-4 (12)	0.0006±0.0708+0.4846±0.0340 [Fe (II)] mmol.L^{-1}	0.9951,0.9902, 99.02	2.228 << 31.749	
Dynamic range or analytical range	0.1-15 (18)	512.8604±387.8074+352.5874±71.3613 [Fe (II)] mmol.L^{-1}	0.9342,0.8727, 87.27	2.120<< 10.475	
	0.1-4.5 (13)	0.0378±0.1087+0.4498±0.0461 [Fe (II)] mmol.L^{-1}	0.9883,0.9767, 97.67	2.201 << 21.460	
Scatter plot	0.1-25 (20)	1011.8339± 523.2435+201.1596±59.3107 [Fe (II)]mmol.L^{-1}	0.8592, 0.7383 , 73.83	2.101 << 7.126	
	0.1-5 (14)	0.0814±0.1440+0.4133±0.0547[Fe (II)] mmol.L^{-1}	0.9786, 0.9577, 95.77	2.179 << 16.4763	

n: no. of measurement, $\hat{Y}_{Zi}$ (mV); estimated response(n=3) in mV for developed method, r: correlation coefficient, r^2: coefficient of determination, R^2% (percentage capital R-squared): explained variation as a percentage / total variation, t_{tab} =$t_{0.05/2,n-2}$ and volume of measuring cell 1 ml for UV-SP

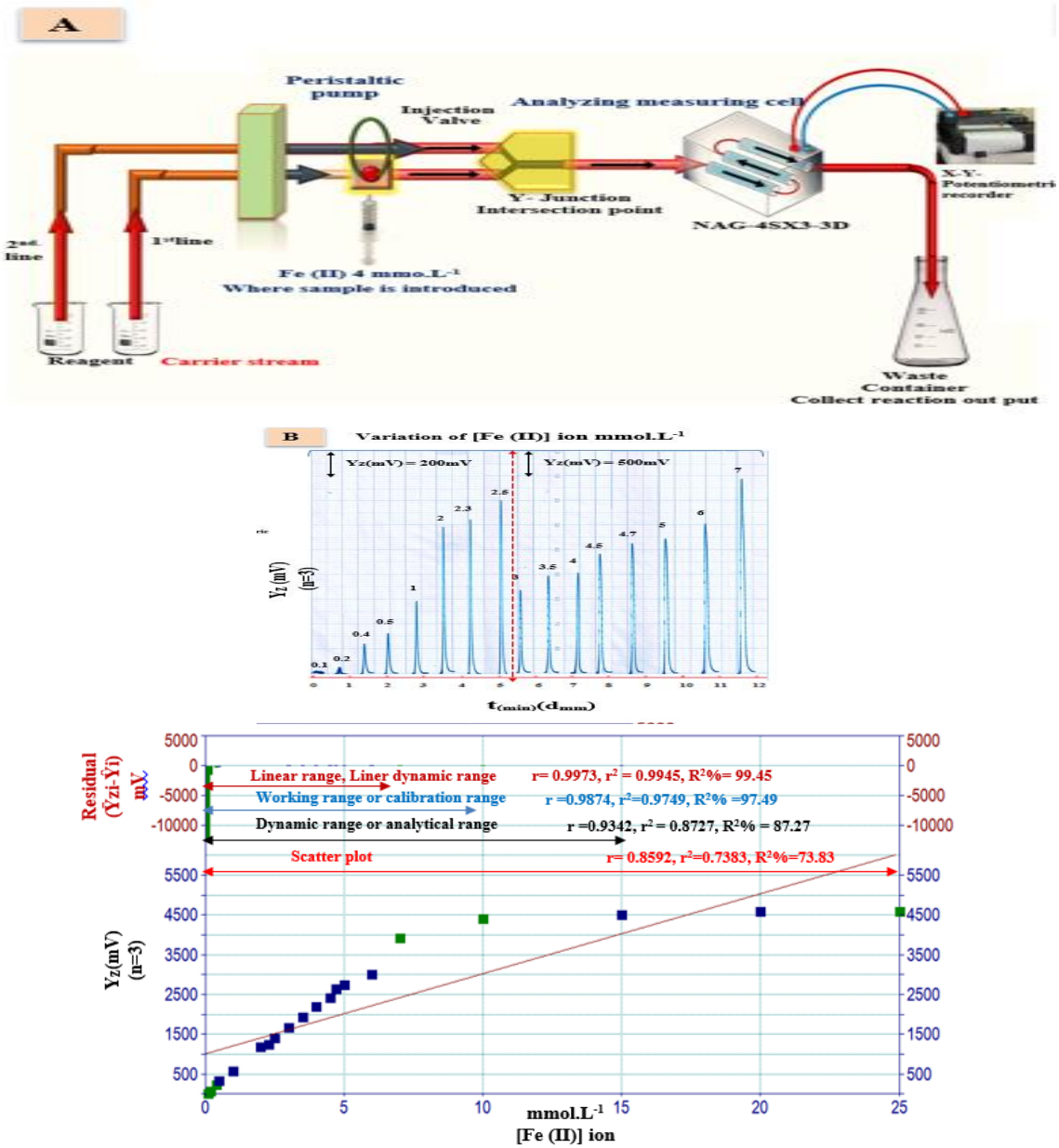

Fig. 4: A: Flow gram system used for the determination of [Fe (II)] ion. B: Some of profiles versus time, potentiometric scanning speed 1cm.min$^{-1,}$ C: Different range for the effect of Fe (II) ion concentration on attenuation of incident light using NAG-4SX3-3D for cell A: scatter plot range (0.1-25) mmol.L^{-1} for n=20, dynamic range (0.1-15) mmol.L^{-1} for n=18, working range (0.1-10) mmol.L^{-1} for n=17 and linear range (0.1-7) mmol.L^{-1} for n=16 against Fe (II) ion concentration, using Fe (II) ion– K_3[$Fe(CN)_6$] (40 mmol.L^{-1}) – CH_3COONH_4 (50 mmol.L^{-1}) system. $\hat{Y}_{Zi}$ (mV); Estimated response (n=3) in (mV) for developed method, r: correlation coefficient, r^2: coefficient of determination, R^2% (percentage capital R-squared): explained variation as a percentage / total variation, $\bar{Y}_{Zi}$ (mV): output (S/N) of energy transducer response in mV.

Table 7: Detection Limit of Fe (II) ion using 175 µL as an injection sample and optimum parameters

Practically, the minuteimum concentration in a scatter plot is based on steady dilution		Theoretical based on the value of slope x=3S_B/slope	Theoretical based on the linear equation $\hat{Y} = Y_b + 3Sb$	Limit of quantitative L.O. Q $\hat{Y}=Y_b+10S_b$
Newly developed method (0.008)mmol.L^{-1}	Classical method (0.005) mmol.L^{-1}			
212.6712 ng/sample	7.5954µg/ sample	0.08865954µg/ sample	13.23705954 µg/ sample	44.12345954 µg/ sample

$\hat{Y}$: Estimated response (mV), X :value of LOD based on the slope(depend on analytical range) , S_B :standard deviation of blank(n=13), Y_b: average response for blank= intercept (a), S_b: standard deviation equal to $S_{y/x}$ (residual), (LOD depend on linear equation of linear range due to low $S_{y/x}$) .

6. Limit of detection (LOD)

Using three different approaches methods as shown in table (7) [24]

7. Repeatability

The accuracy reached by the whole test technique (figure. 5) is calculated by averaging measurements of two Fe (II) ion concentrations, each repeated seven times. This means the relative standard deviation was less than one percent. Figure 5 depicts a response profile for the concentrations utilized.

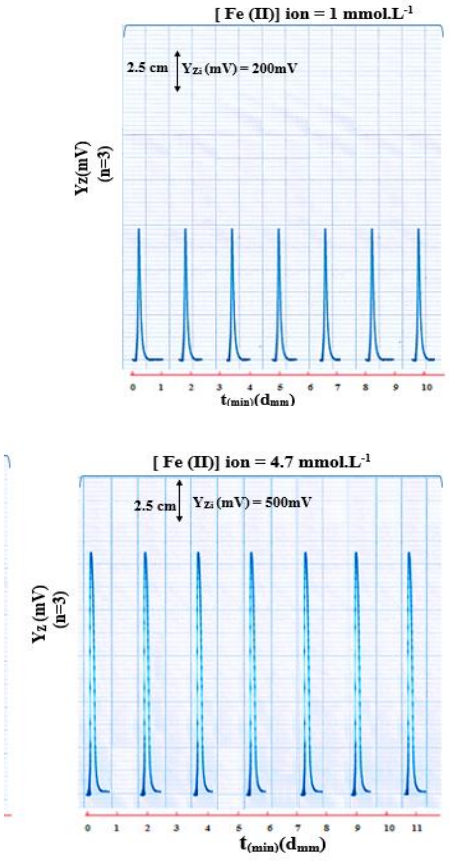

Fig.5: $\bar{Y}_{Zi}$ (mV) – $t_{(Sec)}(d_{mm})$ profile of seven successive measurement with a repeatability of profile for 1and 4.7 mmol.L^{-1} concentration of [Fe(II)]ion using potassium hexacyanoferrate (III) (40 mmol.L^{-1}), using 175 µL as injection loop and 2.5 ml.min^{-1} flow rate for each line

8. Determination of ferrous ion in drugs using a homemade NAG-4SX3-3D analyzer

The approach that has been established was used for the determination of Fe(II) ion in four different kind of Fe(II) ion from four well known drug manufactures (Ferrous sulfate, 200 mg, actives), (FEFOL, 150 mg, MEDIA) , (FE- Folic, 150 mg, BRAWN) and (Fol Iron, 150 mg, pyxus) using NAG-4S3X-3D analyser and compared with classical spectrophotometric method against the measurement of λ_{max} at 222nanometre (figure.6).

Preparing a series of solutions from each medicinal substance was used as the standard addition approach. The measurements were conducted by both methods. A series of Fe(II) ion solution were prepared of pure formulation (Ferrous sulfate) 0.01 mol.L^{-1} , first adding 1 ml to each of the five volumetric flasks (10 ml), then gradually increasing the capacity of each flask (250 mmol.L^{-1}) standard Fe(II) ion (0, 0.04, 0.06, 0.08 and 0.1) ml which equivalent to (0, 1, 1.5, 2 and 2.5) mmol.L^{-1} for both NAG-4SX3-3D analyser and classical UV-Spectrophotometric method. Flask no.1is the sample figure.7 shows the response profile for this study. Table 11.A summarizes the findings of the standard additions technique for the four samples based on the quantity of Fe (II) ion in pharmaceutical medication. While the data in table 11.B summarizes the results for two methods, displaying the practical content of active component at a 95% confidence level, determination efficiency, and paired t-test for comparison of two pathways.

Individual paired t-test ; a comparison of the newly developed approach to the official quoted value μ_0 (150 mg for MEDIA-jordan, BRAWN-India and pyxus-India, and 200 mg for actavis-UK as shown in table 11.A by calculated t_{cal} of each individual company a hypothesis can be estimated as follow:-

H_o (Null hypothesis)**:** for sample no. 1: $\mu_0 = \underline{W}_1$ for actavis- UK

for sample no. 2: $\mu_0 = \underline{W}_2$ for MEDIA-jordan

for sample no. 3: $\mu_0 = \underline{W}_3$ for BRAWN- India

for sample no. 4: $\mu_0 = \underline{W}_4$ for pyxus-India

i.e: There is no significant difference between the means of practical content for four different companies ($\underline{W}_i$) and quoted value (μ_0 = 200 mg or 150 mg)

Against

H_1 (alternative hypothesis): $\mu_0 \neq \underline{W}_i$ for four different companies

i.e: There is a significant difference between the quoted value and means of practical content for four different companies.

For the result obtained that there is $t_{tab} > t_{cal}$ at 95 % confidence level for four drugs, which means no significant different between the quoted value (150 mg or 200 mg) and calculated t-value.

Secondary paired t- test: By combining a created way of analysis (i.e., utilizing the NAG-4SX3-3D analyser) with a traditional approach, a paired t-test was performed across samples from four distinct organizations (i.e: UV-spectrophotometric). Considering individual differences between manufacturers.

A hypothesis can be estimated as a follow:

Null hypothesis H_o : $\mu_{\text{NAG-4SXS-3D analyzer}} = \mu_{\text{UV Spectrophotometric}}$

Agnist

Alternative hypothesis H_1: $\mu_{\text{NAG-4SXS-3D analyzer}} \neq \mu_{\text{UV-Spectrophotometric}}$

Since calculation t_{cal} of 1.8472< 4.303 at 95 % confidence level. Therefore; H_0 is accepted against H_1

i.e.: that there is no significant difference between two methods.

Individual paired t-test: Developed method (NAG-4SX3-3D-CFI Analyzer) there is no significant difference between the means for ferrous (II) ion for four samples and theoretical value, i.e.: H_o is accepted

In addition, take use of the benefits of employing the f-test (scheme 2) to determinate which approach is more exact than others. The established new attained approach is considerably more exact than the ordinary classical method stated in the referenced literature [classical method], according to the results of Scheme 2.Since, variation of newly developed method (S_1^2=501.191) lower than a variant of the traditional approach (S_2^2=577.710)

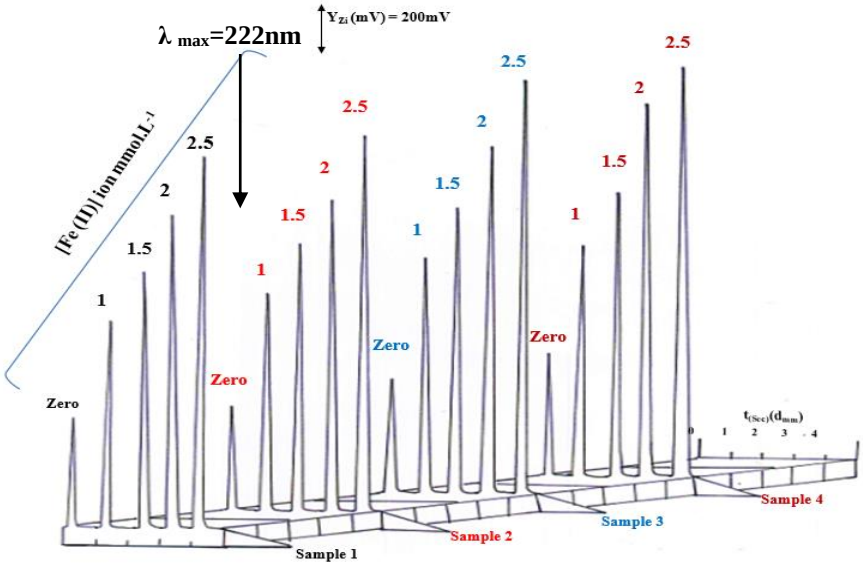

Fig.6: Absorbance of the Fe (II) ion's UV spectrum at a concentration of 2 mmol.L^{-1} with a maximum of 222 nm

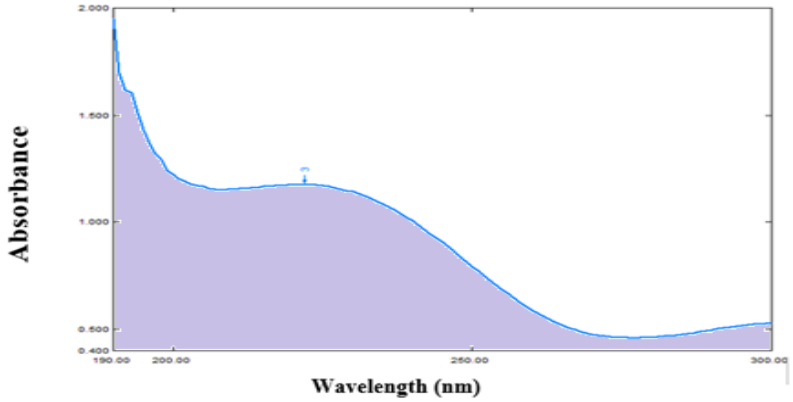

Fig.7: Profile – time for standard addition method using four different companies:
Sample 1: Ferrous sulfate, 200 mg, actavis, UK
Sample 2: FEFOL, 150mg, MEDIA, Jordan
Sample 3: FE-Folic, 150mg, BRAWN, India
Sample 4: FoL Iron, 150 mg, pyxus, India

Table 11.A: Standard addition results for the determination of Fe (II) in four samples of drug using NAG - 4SX3 - 3D analyzer for developed method and UV- Spectrophotometer method (Classical method)

No. of sample	Commercial Name, Company Content Country	Type of method: Developed method using NAG - 4SX3 - 3D analyzer (mV); UV- Spectrophotometer at λ_{max}= 222nm.									
		Confidence interval For the average weight of Tablet $\bar{w}i \pm 1.96\ \sigma_{n-1}/\sqrt{n}$ at 95% (g)	Weight of Sample equivalent to 0.1519 gm (10 mmol.L^{-1}) of the active ingredient W_i(mg)	Theoretical content for the active ingredient at 95% (mg) $Wi \pm 1.96\ \sigma_{n-1}/\sqrt{n}$	[Fe(II)] mmol.L^{-1}					Equation of standard addition at 95% for n-2	r r^2 R^2%
					0	0.04ml	0.06 ml	0.08 ml	0.1ml	$\hat{Y}_i$(mV)=a±s_at+b±s_bt [Fe(II)]mmol.L^{-1}	
					0	1	1.5	2	2.5	$\hat{Y}_i$=a±s_at+b±s_bt [Fe(II)]mmol.L^{-1}	
1	**Ferrous sulfate actavis Fe(II)=200mg UK**	**0.4457±0.0071**	**0.3385**	**200±3.2057**	**465**	**880**	**1080**	**1340**	**1592**	$\hat{Y}_{Zi}$(mV)=443.2160±80.9851+448.703±49.2857[Fe(II)]mmol.L^{-1}	**0.9982** **0.9964** **99.64**
					0.56	**1.06**	**1.34**	**1.63**	**1.92**	$\hat{Y}_{Zi}$=0.5392±0.0633+0.5449±0.0386 [Fe(II)]mmol.L^{-1}	**0.9993** **0.9985** **99.85**
2	**FEFOL MEDIA Fe(II)=150 mg Jordan**	**0.4586±0.0029**	**0.4644**	**150±0.9437**	**450**	**940**	**1140**	**1336**	**1600**	$\hat{Y}_{Zi}$(mV)=461.4590±66.0075+451.2430±40.1670[Fe(II)]mmol.L^{-1}	**0.9988** **0.9977** **99.77**
					0.51	**1.10**	**1.33**	**1.60**	**1.84**	$\hat{Y}_{Zi}$=0.5332±0.0748+0.5305±0.0455 [Fe(II)]mmol.L^{-1}	**0.9989** **0.9978** **99.78**
3	**FE-FOLIC BRAWN Fe(II)=150mg India**	**0.4556±0.0037**	**0.4614**	**150±1.2182**	**500**	**1010**	**1220**	**1480**	**1760**	$\hat{Y}_{Zi}$(mV)=497.0270±56.6428+497.8380±34.4716 [Fe(II)]mmol.L^{-1}	**0.9993** **0.9986** **99.86**
					0.37	**1.21**	**1.24**	**1.46**	**1.68**	$\hat{Y}_{Zi}$=0.4935±0.4070+0.4989±0.2477 [Fe(II)]mmol.L^{-1}	**0.9654** **0.9319** **93.19**
4	**FOLIRON Pyxus Fe(II)=150mg India**	**0.5795±0.0069**	**0.5869**	**150±1.7878**	**530**	**998**	**1220**	**1592**	**1745**	$\hat{Y}_{Zi}$(mV)=514.9190±147.5525+501.4860±89.7960[Fe(II)]mmmol.L^{-1}	**0.9953** **0.9906** **99.06**
					0.54	**1.04**	**1.33**	**1.58**	**1.86**	$\hat{Y}_{Zi}$=0.5303±0.0391+0.5284±0.0239 [Fe(II)]mmol.L^{-1}	**0.9997** **0.9994** **99.94**

$\hat{Y}_{Zi}$: Response in mV for the developed technique and without unit for the UV-Sp. method., r: correlation coefficient, r^2: coefficient of determination, R^2% (R-squared as a percentage): Variation clearly explained as a percentage / total variable, t_{tab}= $t_{0.5/2,\infty}$=1.96 at 95%, t_{tab}= $t_{0.05/2,3}$=3.182 for n=5, UV –Sp.: UV –Spectrophotometric method, using volume of cell (quartz) 1 ml in UV–Spectrophotometric method.

Table 11.B: Summary of results for practical content, efficiency (Rec percent) for determining Fe (II) ion in three drug samples, and t-test for comparing two techniques

No. of sample	Type of method: Developed method using NAG - 4SX3 - 3D Analyzer; UV- Spectrophotometer at λ_{max}= 222nm.			Individual t-test between claimed value & practical value ($\bar{W}_{i(mg)}-\mu$) $\sqrt{n}$ /σ_{n-1}	Paired t –test Compared between three methods	
	Practical concentration (mmol.L^{-1}) in 10 ml Practical concentration (mmol.L^{-1}) in100 ml Practical weight of Fe(II)ion in (g)	Weight of Fe(II)ion in each sample (g) $\bar{W}_{i(g)} \pm 4.303\ \sigma_{n-1}/\sqrt{n}$ Weight of Fe(II)ion in tablet $\bar{W}_{i(mg)} \pm 4.303\sigma_{n-1}/\sqrt{n}$	Efficiency of determination Rec.%		t_{cal}= $\bar{w}d\ \sqrt{n}\ /\sigma^{*}_{n-1}$	t_{tab} at 95%confidence level (n-1)
1	0.9878 9.8777 0.15005	0.15005±0.0037 197.5530±4.8320	98.78%	/-2.179/< 4.303	Newly developed methodology and quoted value (reference method) $\bar{X}d$ = -1.678 σ^{*}_{n-1}= 3.7600 /- 0.8926/ < 3.182	
	0.9896 9.8958 0.15032	0.15032±0.0025 197.915± 3.2820	98.96%			
2	1.0226 10.2264 0.15535	0.15535± 0.0044 153.3940 ± 4.3250	102.26%	3.3767< 4.303		
	1.0051 10.0510 0.1527	0.1527 ± 0.0018 150.764±1.789	100.51%			
3	0.9984 9.9837 0.15166	0.15166±0.0013 149.7560±1.235	99.84%	/-0.8502/< 4.303	Newly developed methodology and UV-spectrophotometric (classical method) $\bar{X}d$ =2.2803 σ^{*}_{n-1}= 2.4563 1.8566 < 3.182	
	0.9892 9.8917 0.1503	0.1503±0.0024 148.3750±2.3280	98.92 %			
4	1.0270 10.2680 0.1560	0.15160±0.0031 156.0090±3.2150	102.70%	0.2742 < 4.303		
	1.0036 10.0358 0.1525	0.1525±0.0024 150.5370±2.38	100.36%			

μ: claim value (200mg& 150 mg), $\bar{w}i$: practically weight in mg, $\bar{X}d$: average of difference between two type of method (developed & classical), $\sigma_{n-1:}$ standard deviation of different (paired t-test), n :(no. of sample) = 4, $t_{tab}=t_{0.05/2,2}$=4.303 (for individual t-test & paired t-test), classical method: UV–Spectrophotometric method.

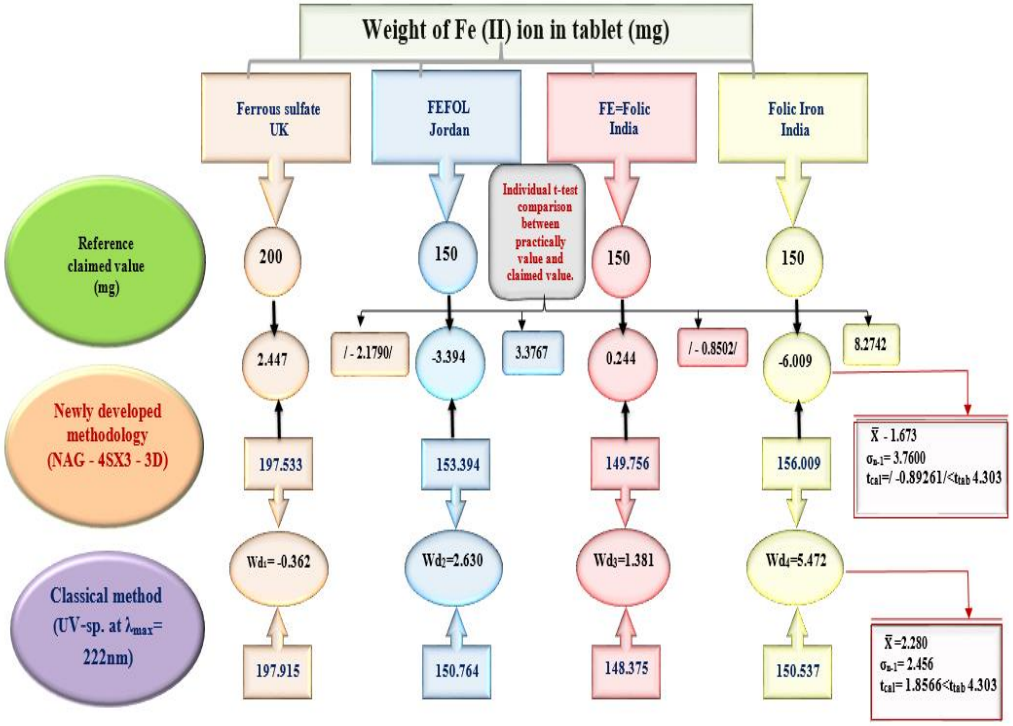

Scheme 2: Set of results for comparison between practically content and claimed valve (Individual t-test) and a comparison of two techniques (Paired t-test), in addition to F-test. t_{tab} =$t_{0.025,2}$=4.303, F_{tab}=$F_{0.95,\upsilon1,\upsilon2}$=$F_{0.95,1,3}$= 10.13, $\overline{Wd}$: the average of the two approaches' differences (developed & classical), Wd: different between two methods ,σ^{*}_{n-1}: the difference standard deviation (paired t-test), σ_{n-1}: standard deviation for Individual t-test.

4. A.4.1. Statistically data treatment using analysis of variance one way- ANOVA

One way ANOVA treatment that is used to compare three or more means but it contains only one variable was used. Assessment of NAG- 4SX3-3D analyzer via the via reaction of Fe (II) ion with $K_3[Fe(CN)_6]$ in the presence of CH_3COONH_4 for analysis of Fe (II) in different pharmaceutical and compared with two classical method (i.e., official method & UV-spectrophpotometric method)(scheme 4.3).

Assumption for the F- test when three or more means are compared. The first estimate is called variance between – groups (SSB) or (SB2). The second estimate, the within-group variance (SSW) or (SW2), is calculated using data and is unaffected by mean differences. (i.e.Si2 = σ n-12).

If there are no variations in the means, the variance between groups will be significantly greater than the variance within groups.

The F- test , the value will be higher than 1 and the null hypothesis would be rejected and accepted alternative hypothesis, the approach is known as analysis of variance "ANOVA". [26-28]

ANOVA test was applied at α= 0.05 (95% confidence level). ANOVA hypothesis testing and sample comparison of ferrous ion are given in table 12.

The first hypothesis (Null hypothesis) (H_0)

H_0= μ activist –UK sample =μ MEDIA –Jordan= μ BRAWN-India= μ pyxus – India

Means there is no significant difference between all used mean of each samples from different companies concerning the output results. The alternative proposed is that there is a significant difference between all mean of values.

H_1 (alternative hypothesis)

H_1: μ activist – UK sample≠ μ MEDIA-Jordan ≠ μ BRAWN-India ≠ μ pyxus - India

The result obtain that were summarized in table 12 shown that no substantial difference exists between the means of each samples gotten from all data, the value of F_{Cal} (1.1527) < F_{tab} (10.13).

Consequently, the alternative hypothesis will be rejected, whereas the null hypothesis will be accepted. This means that for four samples, there is no clear differentiation between four distinct firms.

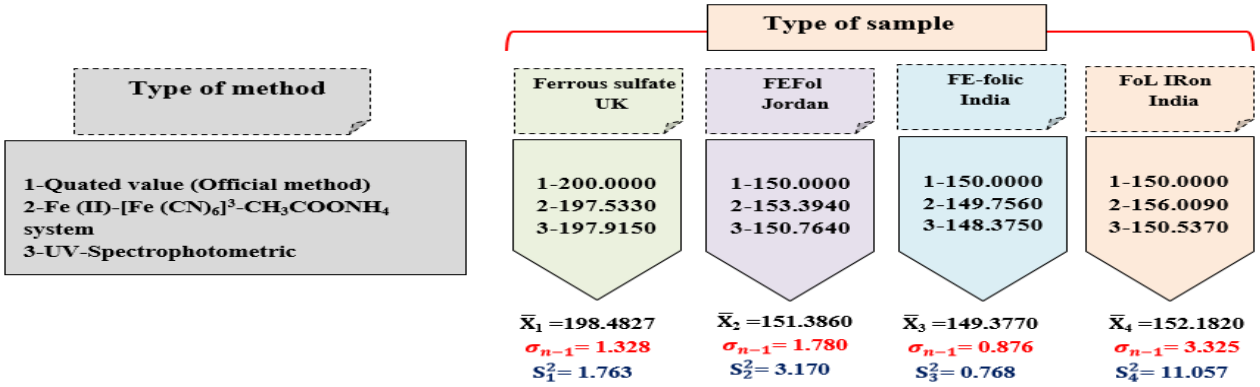

Scheme 4.3: Summed up the results for two different methods in addition to quoted value and four different samples for ANOVA, $\bar{X}$: average of values, σ_{n-1}: standard deviation, s^2= variance

Table 12: ANOVA results for comparison between two different samples from four different Companies

Source	Total of squares (SSq)	Df	Squared mean (MSq)	F_{cal}	$F_{critical}$
Between group	SS_B=5089.314	3	MS_B=1696.438	404.9357 > 4.066181	
Within groups	SS_W=33.51521	8	MS_W=4.18940		
Total	5122.829	11			

df = degree of freedom , F_{tab}= F $_{0.95,V1,V2}$= F $_{0.95,2,9}$= 4.066 at 95% confidence level, K= number of group =4, N=number of measurements or sum of the samples for the groups (i.e) =n_1+n_2+……+n_i =12 , SS_B = The total of squares between group , SS_W = The total of squares within group, MS_B = SS_B/ K-1 & MS_W = SSw/ N-K, F_{cal} = MS_B / **MSw**

CONCLUSION

In comparison to the classical approach, the suggested method employs less expensive apparatus and reagents.

Using the NAG-4SX3-3D analyser, a more effective and quicker determination was accomplished in this research. For all samples, the RSD % was less than 1 %, indicating that the suggested approach is accurate sufficient. The standard addition approach was utilized, to prevent the matrix effect. This approach may also be used to determine ferrous ion in pure and pharmaceutical formulations, it also offers the advantage of excellent sensitivity is achieved without the need for heating or extraction. The results of the statistical analysis are consistent with those obtained using the traditional method.

ACKNOWLEDGMENT

Prof. Issam Mohammad Ali Shakir and Prof. Nagham Skakir , I'd like to express my deepest thanks for giving me the incredible opportunity to conduct this study and for aiding me in its completion.

Conflicts of interest

"There are no conflicts to declare".

REFERENCE

1. K. Hans Wedepohl The composition of the continental crust. , 59(7), 1217–1232. , (**1995**). Doi: 10.1016/0016-7037(95)00038-2
2. Morel, F. M. M. , The Biogeochemical Cycles of Trace Metals in the Oceans. , 300(5621),944947.(2003). Doi:10.1126/science .1083545.
3. Zhu, Xunchi; Zhang, Ruifeng; Liu, Sumei; Wu, Ying; Jiang, Zengjie; Zhang, Jing, Seasonal distribution of dissolved iron in the surface water of Sanggou Bay, a typical aquaculture area in China. Marine Chemistry, 189, 1–9, (**2017**).. Doi:10.1016/j.marchem.2016.12.004.
4. Su, Han; Yang, Rujun; Zhang, Aibin; Li, Yan , Dissolved iron distribution and organic complexation in the coastal waters of the East China Sea. Marine Chemistry, 173, 208–221. (**2015**). Doi:10.1016/j.marchem.2015.03.007.
5. Guan, Jiunian; Yan, Baixing; Zhu, Hui; Wang, Lixia; Lu, Duian; Cheng, Long , Flux characteristics of total dissolved iron and its species during extreme rainfall event in the midstream of the Heilongjiang River. Journal of Environmental Sciences, 30, 74–80. (**2015**). Doi:10.1016/j.jes.2014.10.009.

6. Abduljabbar, Tharwat N.; Sharp, Barry L.; Reid, Helen J.; Barzegar-Befroeid, Neda; Peto, Tunde; Lengyel, Imre , Determination of Zn, Cu and Fe in human patients' serum using micro-sampling ICP-MS and sample dilution. Talanta, S0039914019305922–.,(2019). Doi:10.1016/j.talanta.2019.05.098
7. Feist, Barbara; Sitko, Rafal , Method for the determination of Pb, Cd, Zn, Mn and Fe in rice samples using carbon nanotubes and cationic complexes of batophenanthroline. Food Chemistry, S030881461732054X–.(**2017**). Doi:10.1016/j.foodchem.2017.12.082.
8. Kasa, Nursu Aylin; BakÄ±rdere, Eminutee GÃ¼lhan , Determination of Iron in Licorice Samples by Slotted Quartz Tube Flame Atomic Absorption Spectrometry (FAAS) with Matrix Matching Calibration Strategy after Complexation with Schiff Base Ligand-Based Dispersive LiquidâLiquid Microextraction. Analytical Letters , 1–11. (**2020**). Doi:10.1080/00032719.2020.1801709.
9. Sixto, Alexandra; Mollo, Alicia; Knochen, Moisés , Fast and simple method using DLLME and FAAS for the determination of trace cadmium in honey. Journal of Food Composition and Analysis, S0889157518311803–.(2019). Doi:10.1016/j.jfca.2019.06.001.
10. de Oliveira Souza, Murilo; Ribeiro, Maria Aparecida; Carneiro, Maria Tereza Weitzel Dias; Athayde, Geisamanda Pedrini Brandão; de Castro, Eustáquio Vinícius Ribeiro; da Silva, Francisco Luan Fonseca; Matos, Wladiana Oliveira; de Queiroz Ferreira, Rafael , Evaluation and determination of chloride in crude oil based on the counterions Na, Ca, Mg, Sr and Fe, quantified via ICP-OES in the crude oil aqueous extract. Fuel, 154, 181–187. (**2015**). Doi:10.1016/j.fuel.2015.03.079.
11. Peng, Bo; Chen, Guorong; Li, Kai; Zhou, Minute; Zhang, Ji; Zhao, Shengguo , Dispersive liquid-liquid microextraction coupled with digital image colorimetric analysis for detection of total iron in water and food samples. Food Chemistry, 230, 667–672. (**2017**). Doi:10.1016/j.foodchem.2017.03.099.
12. Zvěřina, Ondřej; Kuta, Jan; Coufalík, Pavel; Kosečková, Pavlína; Komárek, Josef , Simultaneous determination of cadmium and iron in different kinds of cereal flakes using high-resolution continuum source atomic absorption spectrometry. Food Chemistry, 298, 125084–. (**2019**). Doi:10.1016/j.foodchem.2019.125084.
13. Leao, Danilo J.; Junior, Mario M.S.; Brandao, Geovani C.; Ferreira, Sergio L.C., Simultaneous determination of cadmium, iron and tin in canned foods using high-resolution continuum source graphite furnace atomic absorption spectrometry. Talanta, S0039914016300911–. (**2016**). Doi:10.1016/j.talanta.2016.02.023.
14. Borzoei, Mohammad; Zanjanchi, Mohammad Ali; Sadeghi-aliabadi, Hojjat; Saghaie, Lotfollah , Optimization of a methodology for determination of iron concentration in aqueous samples using a newly synthesized chelating agent in dispersive liquid-liquid micro extraction. Food Chemistry, S0308814618307830–. (**2018**). Doi:10.1016/j.foodchem.2018.04.135.
15. Horstkotte, Burkhard; Chocholouš, Petr; Solich, Petr , Large volume preconcentration and determination of nanomolar concentrations of iron in seawater using a renewable cellulose 8-hydroquinoline sorbent microcolumn and universal approach of post-column eluate utilization in a Lab-on-Valve system. Talanta, , S0039914015305725–.(**2015**). Doi:10.1016/j.talanta.2015.12.044.
16. Jamali, Mohammad Reza; Tavakoli, Maedeh; Rahnama, Reyhaneh , Development of ionic liquid-based in situ solvent formation microextraction for iron speciation and determination in water and food samples. Journal of Molecular Liquids, 216, 666–670. (**2016**). Doi:10.1016/j.molliq.2016.02.003.
17. Al-Thakafy, N., Al-Enizzi, M., Saleh, M. (2022). Synthesis of new Organic reagent by Vilsmeier – Haack reaction and estimation of pharmaceutical compounds (Mesalazine) containing aromatic amine groups. *Egyptian Journal of Chemistry*, 65(6), 685-697. doi: 10.21608/ejchem.2021.101851.4729
18. Qusay Falih, I., A.H. Alobeady, M., Banoon, S., Saleh, M. (2021). Role of Oxidized Low-density Lipoprotein in Human Diseases: A Review. *Journal of Chemical Health Risks*, 11(Special Issue: Bioactive Compounds: Their Role in the Prevention and Treatment of

Diseases), 71-83. doi: 10.22034/jchr.2021.684227

19. Issam M. A. Shaki, Zaineb F Hassan, New chemiluminuteometric FIA for pre-absorbed luminuteol in poly acrylic acid gel beads and its use in the determination of Fe(III) ion in an iron or alloys . International Journal of Research in Pharmacy and Chemistry, 5(1),84-94 , ISSN2231-2781. (2015).
20. IRQ. PATENT. No. 6100. Shakir ,I.M.A. and Al-Awadie ,N.S.T., Novel Multiple Continuous Flow Cells (hydrophilic & hydrophobic) works as a Solo Flow cell with Summed S/N responses in NAG- 4SX3 – 3 D. instrument patent, International classification G01N2021/0325 , Iraqi classification 6. (**2020**),
21. sdeek, G., Mauf, R., Saleh, M. (2021). Synthesis and Identification of some new Derivatives Oxazole, Thiazole and Imidazol from Acetyl Cysteine. *Egyptian Journal of Chemistry*, 64(12), 7565-7571. doi: 10.21608/ejchem.2021.88755.4267
22. Hassan, Y. I., & Saeed, N. H. (2010). Kinetic study of chlorination of p-methoxyacetanilide by chloramine-T in hydrochloric acid medium. *Oriental Journal of Chemistry*, *26*(2), 415.
23. Vogel. A.I.1979. A Text book of macro and semi micro Quantitative Inorganic Analysis, 5th ed. Longman group Limited, London.pp:322.
24. Ayoob, A., Sadeek, G., Saleh, M. (2022). Synthesis and Biologically Activity of Novel 2-Chloro -3-Formyl -1,5-Naphthyridine Chalcone Derivatives. *Journal of Chemical Health Risks*, 12(1), 73-79. doi: 10.22034/jchr.2022.688560
25. J.C. Miller & j.N. Miller, Statistics and chemometrics for analytical chemistry. 5th ed., john Wily Sons., New York. , (**2005**).
26. Sawyer, Steven F. , Analysis of Variance: The Fundamental Concepts. Journal of Manual & Manipulative Therapy, 17(2), 27E–38E. (**2009**). Doi:10.1179/jmt.2009.17.2.27e
27. Ruqaya M. Hamid Al-Sultan, Ammar Abdulsalaam Al-Sultan, Mohammed A. Hayawi, Bilal J M Aldahham, Mohanad Y. Saleh, Hazim A. Mohammed. The effect of subclinical thyroid dysfunction on B- type natriuretic peptide level. Revis Bionatura 2022;7(2) 21. http://dx.doi.org/10.21931/RB/2022.07.02.21
28. Toohi, H. T. A. S., Rabeea, M. A., Abdullah, J. A., & Muslim, R. F. (2021). Synthesis and characterization activated carbon using a mix (asphalt-polypropylene waste) for novel azo dye (HNDA) adsorption. *Carbon Letters*, *31*(5), 837-849.